CVEL

THE CLEMSON UNIVERSITY VEHICULAR ELECTRONICS LABORATORY

TECHNICAL REPORT: CVEL-10-022

The Effect of the Vehicle Body on EM Propagation in Tire Pressure Monitoring Systems

Hua Zeng and Dr. Todd Hubing

Clemson University

December 14, 2010

This report was submitted for publication. The revised, peer-reviewed version can be found in the following publication:

H. Zeng and T. Hubing, "The effect of the vehicle body on EM propagation in tire pressure monitoring systems," *IEEE Trans. on Antennas and Propagation*, vol. 60, no. 8, Aug. 2012, pp. 3941-3949.

Table of Contents

Abstract

A typical wireless interface for a Tire Pressure Monitoring System (TPMS) is designed to optimize power transfer in free space without taking the car body into account. Nevertheless, the metal rim of the wheel and the metallic components of the vehicle have a profound effect on the electromagnetic wave propagation between a sensor located in the tire and a receiver mounted on the vehicle chassis. This paper evaluates the vehicle body's effect on tire sensor transmission and propagation; relates these effects to receiver antenna packaging requirements; and describes an antenna design that takes advantage of the car body to improve the efficiency of the power transmission.

1. Introduction

Automatic tire pressure monitoring has been required on all new vehicles sold in the U.S. since September 2007. Most TPMS systems in vehicles today employ battery powered sensors that are mounted in each of the tires and communicate wirelessly with a central unit located behind the dashboard. The batteries in these sensors cannot be replaced; therefore it is necessary to replace the entire sensor module when the battery is too weak to provide a reliable signal. A number of functional issues have been documented with these systems, including false low-pressure warnings that occur when the TPMS signal is lost or interfered with. A significant technical challenge associated with TPMS systems is to ensure adequate and reliable sensor transmission/reception in the vehicle while using the limited sensor power efficiently.

V. Kukshya [1] introduced a system simulator to characterize the performance of tire pressure monitoring systems in various operational scenarios. K. Tanoshita [2] simulated the electric field characteristics of the AIRwatch system in Japan. H. J. Song [3] and M. Brzeska [4] presented RF models for analyzing the signal strength/range of TPMS systems. These results were based on free-space signal propagation between the transmitting module and receiver module. However, in actual implementations, the propagation path from a sensor to a receiver in a TPMS system is not free space. The wheel structure and other metallic components of the vehicle have a profound effect on the propagation characteristics.

This paper examines the factors that affect the communication between TPMS sensors mounted inside a tire and a receiver centrally located in a vehicle. It evaluates the vehicle body's effect on tire sensor transmission and propagation; and shows that TPMS antennas designed to take advantage of the surface waves induced on an automotive chassis can be more effective than TPMS antennas optimized for free space transmission/reception.

2. Maximum EM Transmission/Reception in Free Space

Fig. 1 illustrates the components of the signal path between a transmitter and receiver in free space. The signal path includes a transmitting antenna and its matching network, a receiving antenna and its matching network, and the free space transmission path.

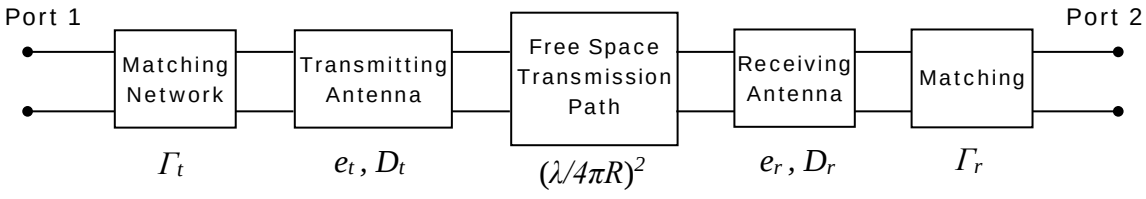

Fig. 1. Signal propagation between a transmitter and receiver in free space.

Assuming the polarization of the receiving antenna is matched to the impinging wave, the power transfer ratio of the received power at Port 2 to the input power at Port 1 can be represented by the product of the contributions from each component of the signal path,

$$\frac{P_r}{P_t} = \left(1-\left|\Gamma_t\right|^2\right) e_t D_t \left(\frac{\lambda}{4\pi R}\right)^2 e_r D_r \left(1-\left|\Gamma_r\right|^2\right) \tag{1}$$

where P_r is the received power delivered to the load; P_t is the input power at the terminals of the matching network; Γ_t and Γ_r are reflection coefficients between the source and the matching network at the transmitting end, and the load and matching network at the receiving end, respectively; e_t and D_t are the radiation efficiency and directivity of the transmitting antenna; e_r and D_r are radiation efficiency and directivity of the receiving antenna; λ is the wavelength and R is the distance between transmitting and receiving antennas. The term $\left(\frac{\lambda}{4\pi R}\right)^2$ is the free space loss factor [5].

If the matching network is ideal (i.e. lossless) and the antennas are aligned for maximum directional radiation and reception, the maximum power transfer can be expressed as,

$$\frac{P_r}{P_t} = e_t e_r D_{0t} D_{0r} \left(\frac{\lambda}{4\pi R}\right)^2 \tag{2}$$

where, D_{0t} and D_{0r} are the maximum directivities of the transmitting antenna and receiving antenna, respectively.

Above an infinite ground plane, the maximum power transfer can be modified by applying image theory,

$$\frac{P_r}{P_t} = e_t e_r Fp \tag{3}$$

where Fp is the *propagation factor*, which is the inversely related to the propagation loss, and can be expressed as,

$$Fp = D_{0t} D_{0r} \left(\frac{\lambda}{4\pi}\right)^2 \left(\frac{1}{R^2} + \frac{1}{R_i^2}\right) \tag{4}$$

where, R_i is the distance between the image of the transmitting antenna and receiving antenna. If the radiation efficiency is unity for both transmitting and receiving antennas, the propagation factor is equal to the power transfer ratio.

For an electrically short linear dipole or a small loop, the maximum directivity occurs in a direction perpendicular to its polarization and has a value of 1.5. In this case, the maximum power transfer ratio at a given frequency only depends on the distances from the transmitting antenna and its image to the receiving antenna. In a TPMS application at 315 MHz, the maximum propagation factor is given by,

$$Fp_{\max} = 0.0129\left(\frac{1}{R^2} + \frac{1}{R_i^2}\right) \tag{5}$$

where the units of R and R_i are meters.

Referring to the two-port network shown in Fig. 1, *Fp* can be expressed in terms of the S-parameters obtained by measurement or simulation.

$$Fp = \frac{S_{21}^2}{\left(1-\left|S_{11}\right|^2\right)\left(1-\left|S_{22}\right|^2\right)\varepsilon_t\varepsilon_r} \tag{6}$$

where $|S_{11}|^2$ is the reflection coefficient at the input to the transmitting antenna's matching network, $|S_{22}|^2$ is the reflection coefficient at the receiver and S_{21} is the transmission coefficient from Port 1 to Port 2. For a particular pair of antennas, the propagation factor is a measure of the quality of EM transmission and reception in the best possible circumstances. For two electrically small antennas, the propagation factor calculated by Eq. (5) is the maximum value that can be obtained in free space over a ground plane.

3. Modeling EM Propagation in a Typical TPMS Application

3.1 Whip Antenna

Most TPMS systems in vehicles today employ a transmitting module mounted in each of the tires that communicates wirelessly with a central receiving unit located behind the dashboard. The transmitting module is normally small relative to a wavelength at the operating frequency. A small whip antenna is often utilized as both the transmitting and receiving antenna because of its relatively high radiation efficiency (compared to other electrically small antennas). For the purposes of this investigation, a typical whip antenna geometry consisting of a piece of metal extending above the surface of a printed circuit board (PCB), as shown in Fig. 2, was modeled. The metal is copper with a conductivity of 5.8e7 S/m. The antenna is driven at one end relative to the circuit board ground and the far end is left open. The antenna height is 10 mm and the length of the antenna is 20 mm. It is implemented close to the edge of the circuit board in order to leave room for the other required circuitry. Full-wave simulation [6] of this structure shows that the radiation efficiency in free space is 88%.

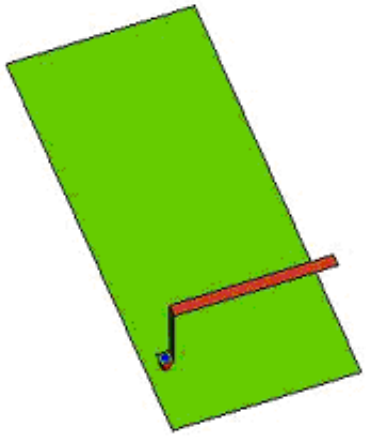

Fig. 2. Geometry of whip antenna

Next, a metal wheel rim is included in the model as shown in Fig. 3. The rim is 6 mm below the PCB with a width of 245 mm and a diameter of 432 mm (17 inches). The PCB is placed near the location of the tire valve. In this configuration, the simulated radiation efficiency decreases to 75%.

Fig. 3. Model for whip antenna on a PCB above a metal rim

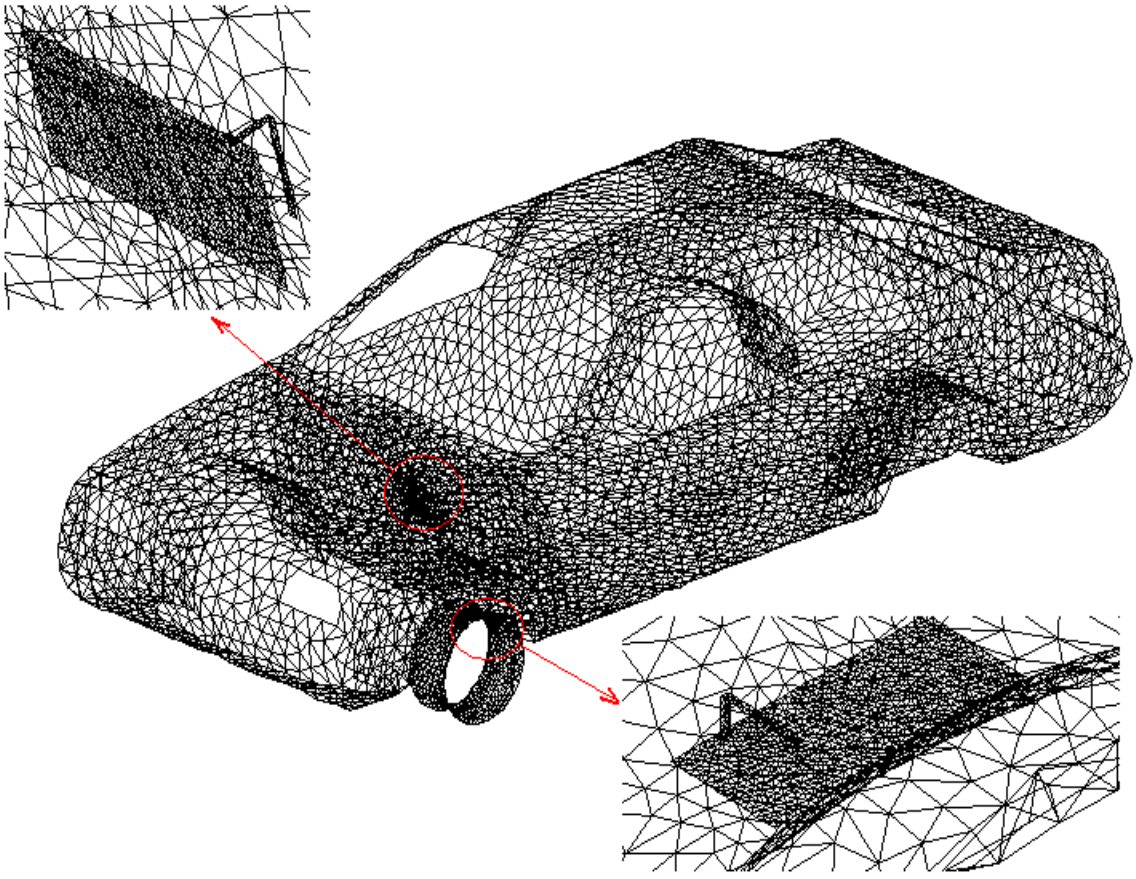

Fig. 4. Model for EM transmission/reception when both rim and car body are taken into account

In order to model the EM transmission/reception in its intended environment, a vehicle body is imported into the model as shown in Fig. 4. The transmitting whip antenna is mounted in the front tire and the receiving whip antenna is located behind the dashboard. The car body and the receiving antenna are symmetric across the width of the vehicle. The car body has a length of 4.6 m, width of 1.8 m, and height of 1.2 m. The distance between two antennas as well as the distance from the image of the transmitting antenna to the receiving antenna are listed in Table 1. These distances were used to calculate the maximum free-space propagation factor Fp_{max} using Eq.(5), which is also listed in Table 1.

Table 1. Maximum propagation factor for two antennas in free space.

Angle	0	45	90	135	180	225	270	315
R (m)	0.9287	1.0183	1.0857	1.0974	1.0482	0.9613	0.8846	0.8701
R_i (m)	1.5316	1.5205	1.4295	1.3029	1.2152	1.2291	1.3339	1.4578
Fp_{max} (10^{-3})	20.49	18.05	17.29	18.35	20.51	22.54	23.78	23.15

Simulations were performed with the wheel in 8 positions from 0 degrees (the antenna at the top of the rim as shown in Fig. 4) to 315 degrees at 45-degree intervals and the S-parameters were calculated. The simulations were performed in three configurations:

Case 1. Between the two antennas in free space above a ground plane;

Case 2. Between the two antennas when the transmitting antenna was mounted on the rim;

Case 3. Between the two antennas when both the rim and car body were present.

The location and orientation of the two antennas were identical in all three cases. The matching network was adjusted for each case to minimize the reflection loss. The matching parameters were determined at the 0-degree position and kept the same when the wheel was rotated. In each case, after the S-parameters and radiation efficiencies were calculated, the actual *Fp* was obtained using Eq. (6) with both radiation loss and reflection loss taken into account. The results are shown in Tables 2 to 4. Although S_{11} theoretically should have its lowest value at 0 degrees, the matching network component values were calculated with finite precision and angles other than 0 degrees sometimes exhibited slightly better matches.

The calculated S-parameters and propagation factor for EM transmission/reception in free space above a ground plane are listed in Table 2. In this case, the propagation factor *Fp* is very close to the maximum possible value Fp_{max} when the transmitter position corresponds to a rim rotation of 45 degrees with only the two antennas present in the model. This is the largest possible propagation factor that can be obtained for the given antenna structure in free space above a ground plane. The rotation of the rim has relatively little effect on the reflection coefficient.

Table 2. Calculated S-parameters and propagation factor for antennas in free space above ground.

Angle	0	45	90	135	180	225	270	315
S_{11}	0.1286	0.193	0.1086	0.1674	0.2522	0.152	0.1326	0.0874
S_{22}	0.0409	0.0458	0.0456	0.0432	0.0415	0.0372	0.0366	0.0427
S_{21}	0.09	0.1150	0.0718	0.0279	0.0373	0.0747	0.0753	0.0163
Fp (10^{-3})	10.65	17.78	6.75	1.04	1.92	7.39	7.46	0.35

Table 3 lists the calculated S-parameters and propagation factor obtained when the rim is included in the simulation. It can be seen that when the antenna position is at 90 degrees, the propagation factor *Fp* is close to the maximum possible Fp_{max}. In this case, the rotation angle has a relatively large effect on the reflection coefficient compared to the free-space case.

Table 3. Calculated S-parameters and propagation factor for antennas with rim present.

Angle	0	45	90	135	180	225	270	315
S_{11}	0.0939	0.2790	0.0876	0.0342	0.3344	0.0952	0.1224	0.1845
S_{22}	0.0218	0.0213	0.0130	0.0154	0.0216	0.0218	0.0218	0.0217
S_{21}	0.0189	0.065	0.0962	0.0871	0.0129	0.0439	0.0136	0.0097
Fp (10^{-3})	0.55	6.95	14.13	11.51	0.28	2.95	0.28	0.15

Table 4 shows the calculated S-parameters and propagation factor when both the front wheel and car body are present. The largest propagation factor Fp occurs when the antenna position is at 45 degrees, and is more than 100 times smaller than the maximum possible Fp_{max} calculated in free space. It is evident that the signal propagation is severely attenuated by the car body. The rotation angle of the wheel has a significant impact on the reflection coefficient of the transmitting antenna.

Table 4. Calculated S-parameters and propagation factor for antennas with rim and car present.

Angle	0	45	90	135	180	225	270	315
S_{11}	0.1715	0.3761	0.2278	0.1385	0.6079	0.1010	0.2355	0.3630
S_{22}	0.0023	0.0002	0.0020	0.0002	0.0023	0.0000	0.0023	0.0001
S_{21}	0.0089	0.0095	0.0055	0.0084	0.0025	0.0089	0.0067	0.0027
Fp^* (10^{-3})	0.11	0.14	0.04	0.09	0.01	0.10	0.06	0.01

* Calculated using Eq. (6).

Similar simulations were performed for the transmitting antenna mounted in the rear wheel. The distance information, calculated S-parameters, and propagation factors are listed in Table 5. The distance between the receiver and the antenna in the rear wheel is around 2.5 times larger than it was when the transmitting antenna was located in the front wheel. The maximum propagation factor for the rear wheel location is about 6 times smaller than it is for the front wheel location in free space above a ground plane. However, when car body is taken into account, the largest propagation factor for the rear wheel is actually around 2 times larger than for front wheel.

Table 5. Relevant parameters for transmitting antenna in the rear wheel.

Angle	0	45	90	135	180	225	270	315
R (m)	2.4589	2.3374	2.3171	2.4125	2.5596	2.6711	2.6886	2.6034
R_i (m)	2.7440	2.5958	2.4968	2.5127	2.6324	2.7787	2.8680	2.8541
Fp_{max} (10^{-3})	3.85	4.28	4.48	4.27	3.84	3.49	3.36	3.49
S_{11}(ant)	0.1265	0.1822	0.1050	0.1686	0.2509	0.1512	0.1332	0.0864
S_{22}(ant)	0.0427	0.0424	0.0422	0.0425	0.0428	0.0423	0.0421	0.0419
S_{21}(ant)	0.0225	0.0092	0.0173	0.0299	0.0233	0.0018	0.0166	0.0252
Fp(ant) (10^{-3})	0.67	0.11	0.39	1.19	0.75	0.01	0.36	0.83
S_{11}(ant+rim)	0.0943	0.2754	0.0795	0.0415	0.3347	0.0958	0.1222	0.1840
S_{22}(ant+rim)	0.0425	0.0425	0.0428	0.0423	0.0425	0.0417	0.0428	0.0425
S_{21}(ant+rim)	0.0144	0.0186	0.0044	0.0269	0.0132	0.0377	0.0133	0.0268
Fp(ant+rim) (10^{-3})	0.32	0.57	0.03	1.10	0.30	2.18	0.27	1.13
S_{11}(ant+rim+car)	0.3115	0.4541	0.2765	0.0858	0.5800	0.1269	0.3055	0.3629
S_{22}(ant+rim+car)	0.0023	0.0006	0.0023	0.0007	0.0022	0.0006	0.0023	0.0005
S_{21}(ant+rim+car)	0.0101	0.0091	0.0096	0.0136	0.0100	0.0108	0.0075	0.0027
Fp(ant+rim+car) (10^{-3})	0.15	0.13	0.13	0.24	0.19	0.15	0.08	0.01

3.2 Loop Antenna

A loop antenna (Fig. 5) was used to receive signals instead of the whip antenna (transmitting antenna was still a whip) and similar simulations for the front wheel were performed. The loop antenna has the same dimensions as the whip antenna except the far end is shorted to the ground plane of the PCB. Full-wave simulation [6] of this configuration indicates the receiving efficiency is 5%.

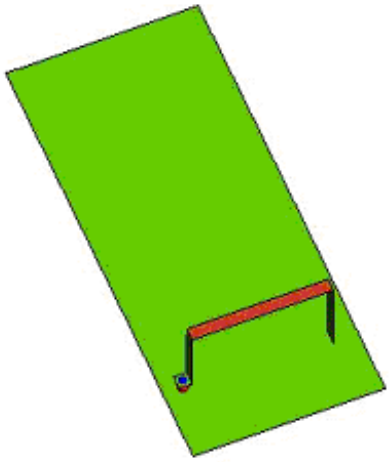

Fig. 5. Geometry of loop antenna

Table 6 shows the calculated S-parameters and propagation factors for EM transmission and reception in the presence of the car body when the loop antenna is used to receive the signal. The largest propagation factor *Fp* occurs when the rim is rotated to 135 degrees. This value is more than 100 times smaller than the maximum possible $Fp_{max.}$

Table 6. S-parameters and propagation factor for EM transmission/reception in the presence of the car body when loop antenna is used for receiving signals.

Angle	0	45	90	135	180	225	270	315
S_{11}	0.0647	0.1467	0.1626	0.2261	0.2858	0.2074	0.0870	0.2277
S_{22}	0.0008	0.0029	0.0008	0.0029	0.0009	0.0029	0.0008	0.0029
S_{21} (10^{-3})	0.48	0.59	1.37	2.42	0.41	1.22	1.50	1.00
Fp (10^{-3})	0.01	0.01	0.04	0.14	0.01	0.04	0.05	0.02

From the simulation results, it is evident that the car body has a significant impact on the propagation factor *Fp* and input impedance of the antenna. Therefore it is better not to optimize EM transmission and reception by designing antennas for free space transmission and reception. A more effective approach is to take advantage of the surface wave of the car body to maximize the propagation factor.

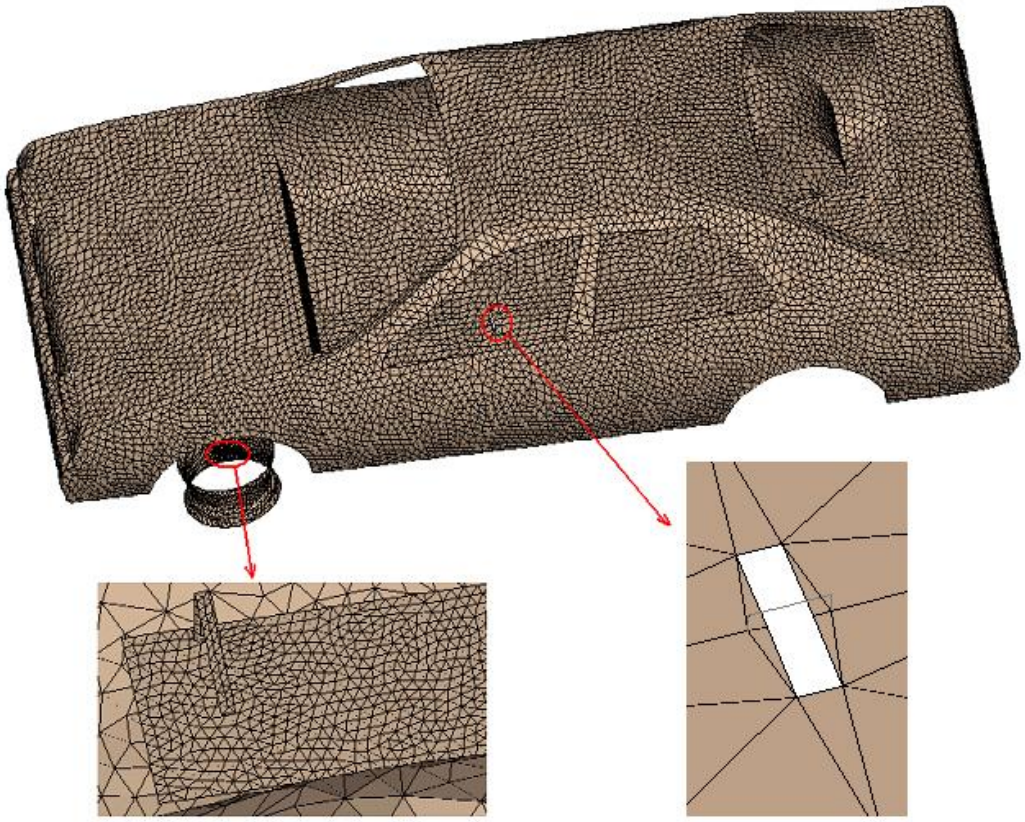

Fig. 6. Whip antenna transmitter and loop-over-slot receiver.

4. Employing Surface Waves to Improve TPMS Efficiency

The car body affects the S_{21} and input impedance of the antenna, thus the propagation factor. Therefore, it is better to optimize antennas for their intended working environment rather than for free-space propagation. By designing antennas to use the car body, the efficiency of the EM communication can be greatly improved. Fig. 6 illustrates an example of an antenna that makes good use of the car body. The transmitting antenna is the same whip antenna used in Section 3; a 20-mm x 5-mm loop antenna located on the bottom metal surface of the car body is used to detect the currents associated with surface waves flowing on vehicle structure. A 40-mm x 10-mm slot is created beneath the loop

antenna to block the currents flowing on the body and increase the current density (i.e. magnetic field strength) around the loop antenna.

Fig. 7 shows the simulated current distribution on the car body. It can be seen that the current density around the slot is much larger than anywhere else.

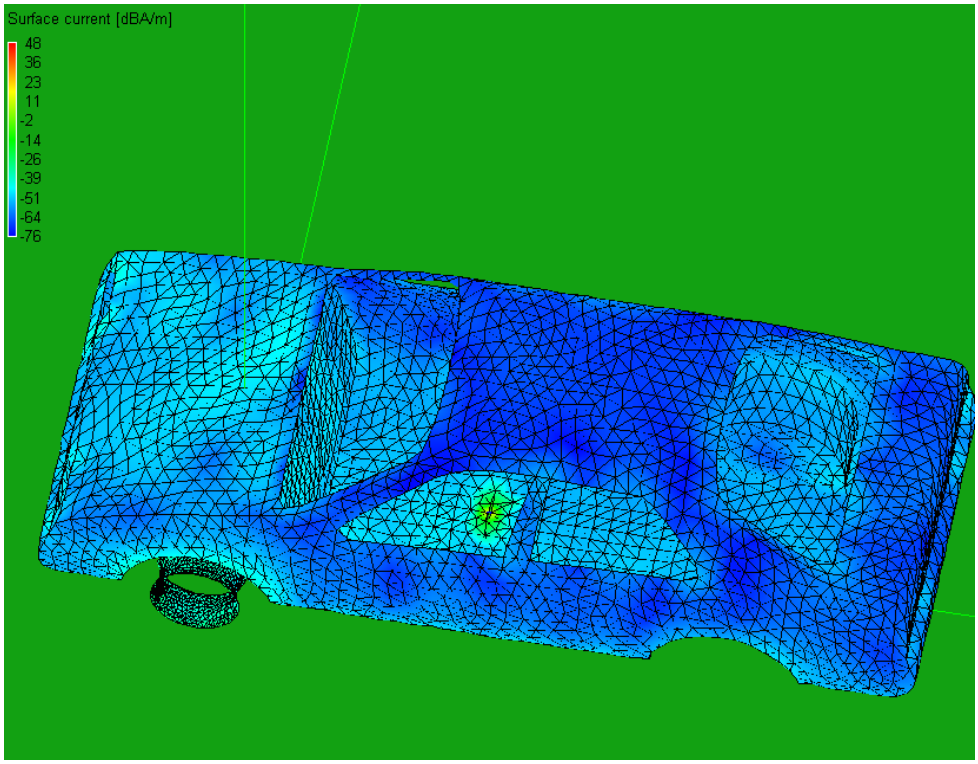

Fig. 7. Current distribution on car body

Table 7 lists the distance information, calculated transmission coefficient, and propagation factors when the wheel is rotated from 0 to 315 degrees at 45-degree intervals. The maximum no-loss propagation factors in free space calculated using Eq.(5), are also listed in the table. When the transmitting antenna position is at 90 degrees, the propagation factor *Fp* is 20.68, which is around 3 times larger than Fp_{max}, and 150 times larger when compared to the results in Table 4 for the traditional model.

Table 7. Distance information, calculated S-parameters and propagation factor for a full turn front wheel.

Angle	0	45	90	135	180	225	270	315
R (m)	1.6519	1.7601	1.7879	1.7223	1.5946	1.4743	1.4404	1.5182
R_i (m)	1.8229	1.8996	1.8823	1.7788	1.6414	1.5520	1.5730	1.6891
Fp_{max} (10^{-3})	8.63	7.75	7.69	8.44	9.88	11.31	11.45	10.14
S_{11}	0.1760	0.3787	0.2357	0.1385	0.6119	0.1015	0.2369	0.3679
S_{22}	0.0087	0.0021	0.0092	0.0010	0.0069	0.0005	0.0028	0.0059
S_{21}	0.0838	0.0475	0.0927	0.0154	0.0730	0.0270	0.0479	0.0761
Fp (10^{-3})	16.47	5.99	20.68	0.55	19.36	1.67	5.53	15.22

Similar simulations were performed when the antenna was mounted in the rear wheel; the distance information, calculated S-parameters, propagation factors, and maximum propagation factors are all listed in Table 8. The largest propagation factor *Fp* is 20.85 and occurs when the antenna is at 225

degrees. This value is around 2.5 times larger than Fp_{max} and 100 times larger when compared to the results in Table 5 for the traditional model.

The largest propagation factor *Fp* for the new design and traditional model in the presence of the car body (blue bar), as well as the corresponding theoretically maximum Fp_{max} (red bar) calculated in free space are plotted in Fig. 8 (for the front wheel) and Fig. 9 (for the rear wheel). In Fig. 8, the propagation factor for the traditional model is plotted after 10 times amplification for display purposes. It is evident that the efficiency of the EM communication is greatly improved by employing the car body as a part of the antenna design.

Table 8. Distance information, calculated S-parameters and propagation factor for a full turn rear wheel.

Angle	0	45	90	135	180	225	270	315
R (m)	1.6107	1.4852	1.4383	1.5047	1.6362	1.7509	1.7896	1.7341
R_i (m)	1.7857	1.6482	1.5541	1.5690	1.6818	1.8168	1.8979	1.8856
Fp_{max} (10^{-3})	9.03	10.62	11.60	10.96	9.40	8.13	7.62	7.93
S_{11}	0.3115	0.4568	0.2788	0.0911	0.5819	0.1351	0.3064	0.3645
S_{22}	0.0084	0.0070	0.0075	0.0082	0.0044	0.0119	0.0085	0.0069
S_{21}	0.0513	0.0566	0.0500	0.0732	0.0278	0.0949	0.0566	0.0532
Fp (10^{-3})	6.62	9.20	6.16	12.28	2.66	20.85	8.04	7.42

Fig. 8. Propagation factor between new designs and traditional model for front wheel

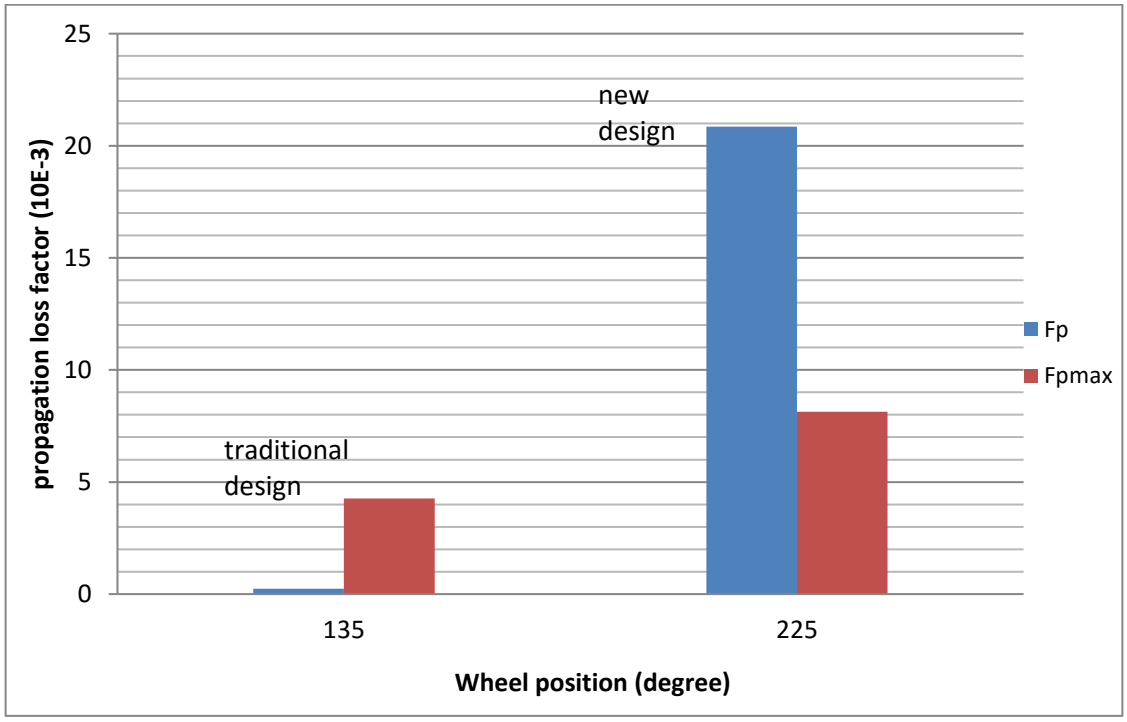

Fig. 9. Propagation factor between new designs and traditional model for rear wheel

Table 9 lists the maximum S_{21} over a full turn for the front wheel when the length of the slot changes from 20 mm to 480 mm. It can be seen that when the slot length is 40mm, which is less than one twentieth of a wavelength, the S_{21} can be as high as 0.09, which is not much less than its value even when the slot length is increased to a half wavelength (λ~1 meter).

Table 9. Transmission coefficients for various slot lengths

Length(mm)	20	30	40	90	120	240	320	480
S_{21}	0.0691	0.0821	0.0927	0.1055	0.1183	0.1241	0.1256	0.1265

Similar simulations were performed at 310 MHz and 433 MHz. The calculated S-parameters and propagation factors are listed in Tables 10 and 11. When the wheel is rotated 90 degrees, the propagation factor *Fp* is at least 2 times larger than Fp_{max}. In other words, small changes in the dimensions of the vehicle relative to a wavelength will not significantly influence the performance of this design.

Table 10. Calculated S-parameters and propagation factors at 310 MHz.

Angle	0	45	90	135	180	225	270	315
Fp_{max} (10^{-3})	8.91	8.00	7.94	8.72	10.20	11.68	11.82	10.47
S_{11}	0.009	0.4098	0.1896	0.2416	0.5093	0.1626	0.1969	0.3649
S_{22}	0.0065	0.0017	0.0059	0.0008	0.0041	0.0009	0.0042	0.0032
S_{21}	0.0807	0.0558	0.0805	0.0317	0.0682	0.0155	0.0655	0.0662
Fp (10^{-3})	15.93	9.15	16.44	2.61	15.40	0.60	10.92	12.36

Table 11. Calculated S-parameters and propagation factors at 433 MHz.

Angle	0	45	90	135	180	225	270	315
Fp_{max} (10^{-3})	4.56	4.10	4.07	4.47	5.23	5.98	6.06	5.36
S_{11}	0.0109	0.2802	0.0529	0.1847	0.2000	0.2316	0.2975	0.0758
S_{22}	0.0040	0.0013	0.0085	0.0004	0.0053	0.0005	0.0027	0.0031
S_{21}	0.0694	0.0433	0.0978	0.0311	0.0714	0.0188	0.0496	0.0614
Fp (10^{-3})	7.75	3.27	15.43	1.61	8.54	0.60	4.34	6.10

5. Conclusions

Ensuring adequate sensor transmission and reception is a key issue faced by TPMS designers. Traditional TPMS systems utilize a transmitting antenna mounted in a tire communicating wirelessly with a central unit mounted behind the dash board. In this paper, a propagation factor was defined to quantify the quality of EM propagation after eliminating the effect of the antenna efficiency and reflection loss. The simulations show that two well positioned and oriented whip antennas can achieve a propagation factor close to the theoretical maximum in free space above a ground plane. However, antennas optimized for free-space transmission exhibited poor performance when the wheel rim and car body were present. With the car body in place, the propagation factor was more than a factor of 100 below the optimum free-space value. It is evident that car body has a significant influence on the efficiency of the power transfer; therefore, it is better not to optimize antenna designs for free-space communication.

A more effective approach is to design antennas that utilize the surface wave propagating on the body of the vehicle. An example design was presented for a receiving antenna employing a 20-mm x 5-mm loop antenna with a 40-mm x 10-mm slot beneath it. Simulations show that this design exhibits a propagation factor 150 times larger than the traditional design. Its propagation factor is 3 times higher than the theoretical maximum free-space value while maintaining the same small size as the traditional design.

References

[1] V. Kukshya, H.J. Song, H.P. Hsu, and R.W. Wiese, "Characterizing performance of tire pressure monitoring systems using experimental measurements and system simulations," *Proc. of 2007 IEEE International Symposium on Antennas and Propagation*, Honolulu, HI, USA, June 2007, pp. 4112-4115.

[2] K. Tanoshita, K. Nakatani, and Y. Yamada, "Electric field simulations around a car of the tire pressure monitoring system," *IEICE Trans. on Communications*, vol. E90-B, no. 9, pp. 2416-2422, Sept. 2007.

[3] H.J. Song, H.P. Hsu, R. Wiese, and T. Talty, "Modeling signal strength range of TPMS in automobiles", *Proc of IEEE International Symposium on Antennas and Propagation*, Sendai, Japan, Aug. 2004, pp. 3167-3170.

[4] M. Brzeska, and G.-A. Chakam, "RF modeling and characterization of a tyre pressure monitoring system," *Proc of 2nd European Conference on Antennas and Propagation*, Edinburgh, UK, Nov. 2007, pp. 1-6.

[5] C.A. Balanis, *Antenna Theory*, New York: Wiley, 2005.

[1] FEKO User Manual, Suite 5.4, 2008.